

## **The effect of PAN or pitch-based C fibres on the microstructure and properties of continuous Cf-ZrB<sub>2</sub>/SiC UHTCMCs**

D. Sciti<sup>1</sup>, L. Zoli<sup>1</sup>, A. Vinci<sup>1</sup>, L. Silvestroni, P. Galizia<sup>1</sup>

<sup>1</sup> *National Research Council, Institute of Science and Technology for Ceramics, Via Granarolo 64, 48018 Faenza, Italy*

### **ABSTRACT**

In this paper the microstructure and thermo-mechanical properties of two different Cf/ZrB<sub>2</sub>-SiC composites reinforced with continuous PyC coated PAN-derived fibres or uncoated pitch fibres were compared.

Pitch-based carbon fibres showed a lower degree of reaction with matrix grains during sintering compared to PyC/PAN-derived fibres. The reason lies in the different microstructure of the carbon. The presence of a coating for PAN-derived fibres was found to be essential to limit the reaction at the fibre/matrix interface during SPS. However, coated bundles were more difficult to infiltrate, resulting in a less homogeneous microstructure.

As far as the mechanical properties are concerned, specimens reinforced with coated PAN-derived fibres provided higher strengths and damage tolerance than uncoated pitch-fibres, due to the higher degree of fibre pull-out. On the other hand, the weaker fibre/matrix interface resulted in lower interlaminar shear, off-axis strength and ablation resistance.

Keywords

UHTCMC, Carbon fibres, mechanical properties, microstructure, self-healing.

### **1. Introduction**

Ultra-high temperature ceramic matrix composites (UHTCMCs) are a novel class of materials obtained from the combination of a UHTC matrix and carbon or silicon carbide fibres/preforms [1], where ultra-high temperature ceramics are borides and carbides of early transition metals [2,3]. The added value of these composites is the possibility to couple the damage tolerance of fibre reinforced composites with the refractoriness of UHTCs.

The target is the achievement of a futuristic generation of reusable materials for application above 2000°C in aerospace, military and nuclear applications [4–10]. This niche of materials has

recently become a new field of research and the latest review papers by L. Rueschoffs et al. [11] and Binner et al. [12] have reported a large escalation of published papers in the last two years. At the moment the research is still very focused on the design and processing of these composites.

The UHTCMC class includes composites with both short and continuous fibres, that can be either SiC<sub>f</sub> or C<sub>f</sub>, although most of the research is focused on C<sub>f</sub> [12]. Preferably, UHTCMCs are constituted of just two essential elements perfectly integrated e.g.: carbon fibres and ultra-refractory matrix (UHTC). The ideal composite has neither a pre-processing fibre coating nor a post processing environmental external coating. Moreover, interface is weak enough to have sufficient fibre pullout at fracture and dense enough to hinder penetration of corrosive/oxidative gases during exposition.

Several processing techniques have been adopted for manufacturing UHTCMCs, most of which are readapted from the CMC science. The most important and studied are:

- polymer infiltration and pyrolysis (PIP), where the UHTC phase is added to a SiC precursor [13]. This method allows the manufacturing of large pieces with complex preforms, but lack of UHTC precursors results in a relatively low content of UHTC phase.
- reactive melt infiltration (RMI), where the carbon preforms are infiltrated with Zr-containing melts [14]: this technique has the advantage to be very fast and versatile, but the Zr based melt easily reacts and degrades the carbon fibres.
- chemical vapor infiltration (CVI) with gaseous precursors of UHT carbide phases, or with C precursors preceded by an infiltration stage with a UHTC containing slurry [15,16]. This is by far the best processing route for achieving large pieces, stress-free composites with a desired weak fibre matrix interface. However, this processing is time consuming and currently densification is mostly achieved by a C gaseous precursor, rather than a UHTC one.

All these methods result in a powdery, non-sintered matrix. An alternative route is manufacturing of UHTCMCs via slurry infiltration and densification by hot pressing or similar consolidation techniques. In a previous paper we demonstrated the feasibility of the SPS process for the consolidation of UHTCMCs, containing either PAN or pitched C fibres [17], which allows to produce composites in very short time. Current limitations for this process are the impossibility to use complex preforms, such as 3D or higher complexity preforms, and formation of strong fibre matrix interface due to the sintering process.

Beside these possible techniques to manufacture UHTCMCs, there is still a lot of variability in the design of these materials, including the matrix composition, the choice of fibre, the fibre volumetric content and architecture. Consequently, data on mechanical properties that correlate properties with the constituent elements of the microstructure are still scarce and scattered.

The scope of this work is to illustrate two examples of UHTCMCs obtained by slurry impregnation and spark plasma sintering (SPS), with the same matrix, but different types of Carbon fibres, e.g. pitch and PAN, to highlight the differences in processing, microstructure and final performance. For the sake of comparison UD composites were produced for mechanical testing.

## 2. Experimental

Commercial products were used for the production of UHTCMCs: ZrB<sub>2</sub> (Grade B, H.C. Starck, Germany, particle size range 0.5-6 μm, impurities (wt%): 0.2 C, 1.3 O, 0.19 N, 0.1 Fe, 1.4 Hf); α-SiC (Grade UF-25, H.C. Starck, Germany, D50 0.45 μm); PAN-derived carbon fibres (T800HB-6000, TORAYCA, Japan), diameter 5 μm, coating: pyrolytic carbon (PyC) 0.0811 g/m (coating thickness ~0.5 μm); pitch-based Cf (XN80-6K, Granoc, Japan), diameter 10 μm, uncoated.

Water-based slurries containing a 90 vol% ZrB<sub>2</sub> - 10 vol% SiC powder mixture were prepared according to previously published procedure [18] and used to impregnate UD preforms, either based on PyC coated PAN fibres or Pitch fibres. Then, impregnated layers were overlapped in 0/0 stacking sequence to get unidirectional composites (UD samples). Detailed compositions were the following:

45 vol% (90 % ZrB <sub>2</sub> -10 % SiC) + 55 vol% PyC-PAN-Cf,	labelled as PAN
55 vol% (90 % ZrB <sub>2</sub> -10 % SiC) + 45 vol% Pitch-Cf,	labelled as PITCH

Discs with diameter  $\varnothing = 40$  mm were then sintered by spark plasma sintering [17] (SPS furnaces HPD25, FCT Systeme GMBH, Germany) under vacuum at 1850°C, with 200 s holding time, 100 °C/min heating rate and 40 MPa applied pressure. The temperature was recorded through a pyrometer placed at the top of the machine and pointing at the centre of the blank (5 mm over the top surface). The bulk density of the sintered pellets was measured using Archimedes' method. The theoretical density of the materials was calculated with the rule of mixtures on the basis of the starting composition. The microstructures were analysed on polished and fractured surfaces using field emission scanning electron microscopy (FE-SEM, Carl Zeiss Sigma NTS GmbH Oberkochen, Germany) to analyse the fibre matrix interface, secondary phases and matrix residual porosity. Residual porosity and average grain size of ZrB<sub>2</sub> were measured by image analysis using the Image-Pro Analyzer 7.0 software (v.7, Media Cybernetics, USA) on SEM images of polished sections.

Four-point bending tests were performed on 25.0 × 2.5 × 2.0 mm<sup>3</sup> bars (length by width by thickness, respectively) at RT ( $\sigma$ ) and 1500 °C in Ar atmosphere ( $\sigma_{1500^\circ\text{C}}$ ) in both longitudinal and transversal directions. Chevron notched beams (CNB) specimens of 25.0 × 2.0 × 2.5 mm<sup>3</sup> (length by width by thickness, respectively) were used for toughness tests ( $K_{Ic}$ ). The test bars were notched with

a 0.1 mm-thick diamond saw; the chevron-notch tip depth and average side length were about 0.12 and 0.80 of the bar thickness, respectively. All tested bars were fractured using a semi-articulated four-point fixture with a lower span of 20 mm and an upper span of 10 mm, using a Zwick-Roell Z050 screw-driven load frame. The crosshead speed was 1 mm/min and 0.05 mm/min for  $\sigma$  and  $K_{Ic}$ , respectively. The Work-of-Fracture (WoF) was calculated from the CNB test as the area below the load-displacement curve divided by the double of the projected real surface. In addition, three-point bending tests were performed on  $25.0 \times 5.0 \times 3.0 \text{ mm}^3$  bars (length by width by thickness, respectively) in order to evaluate the interlaminar shear strength (ILSS) by short beam shear (SBS) test method. A span of 15 mm and a crosshead speed 1 mm/min were used. For each test, at least three bars were used.

The oxidation resistance to dissociated plasma of oxygen and nitrogen was tested through the arc-jet wind tunnel SPES available at the University of Naples “Federico II”. Small sized UHTCMC notional models were machined from both samples and exposed to a supersonic high enthalpy gas mixture of nitrogen (0.8 g/s) and oxygen (0.2 g/s) (nominal Mach number 3). During the test, the arc power of the plasma torch was gradually increased, leading to an increase of pressure and temperature and enthalpy, reaching a maximum value of 20 MJ/kg for 120 s. Further experimental set-up details are reported in dedicated works. [19,20] Post-test analyses were carried out by SEM-EDS analyses.

### **3. Results and discussion**

#### **3.1 Microstructural features**

Microstructural features of the starting fibres and composites are shown in Fig. 1a-f. PyC-coated PAN-based fibres (supplied by AIRBUS DS)  $\phi \sim 5 \mu\text{m}$ , have a turbostratic structure and are quite reactive in the sintering environment with a UHTC matrix. The 400 nm coating applied to limit excessive reaction at the interface is visible in Fig. 1a. Fig. 1a-c show microstructure and interface in the final PAN-composite. When PyC-coated PAN fibres were used, fibre distribution was a partially uneven, Fig. 1b, because the coating procedure caused the fibres to stick together and the liquid slurry could not penetrate the stuck bundles. The fibre volumetric amount was consistent with the designed composition, around 55 vol%, density around  $2.8 \text{ g/cm}^3$  and residual porosity 18% (see Table 1). As for the matrix-fibre interface, the presence of the coating was effective in limiting the carbon reactivity with matrix phases, since it acted as a buffer layer. Spurious phases such as SiC and ZrC phases were detected (see Fig. 1c). As expected, the coating favoured a higher degree of fibre pullout, due to weak interfaces. Pitch-based fibres,  $\phi \sim 10 \mu\text{m}$ , are characterized by a higher degree of graphitization and a typical onion structure Fig. 1d. This structure allowed their use in a severe sintering environment at high temperature and under high pressure even without a protective coating [1,21]. Typical microstructure overview and fibre/interface features are reported in Figs. 1 e,f and

Table 1. PITCH composites had a higher density,  $3.6 \text{ g/cm}^3$ , porosity around 7% and fibre volumetric content in the range 40-45 vol%. The fibres were homogeneously distributed in the matrix, and the fibre/matrix interface was quite smooth. Fibre pullout, though much more limited, was allowed by the intrinsic fibre “onion” structure. Indeed, the external shell was well anchored to the matrix, but pull-out occurred between internal layers, as previously reported [1,21].

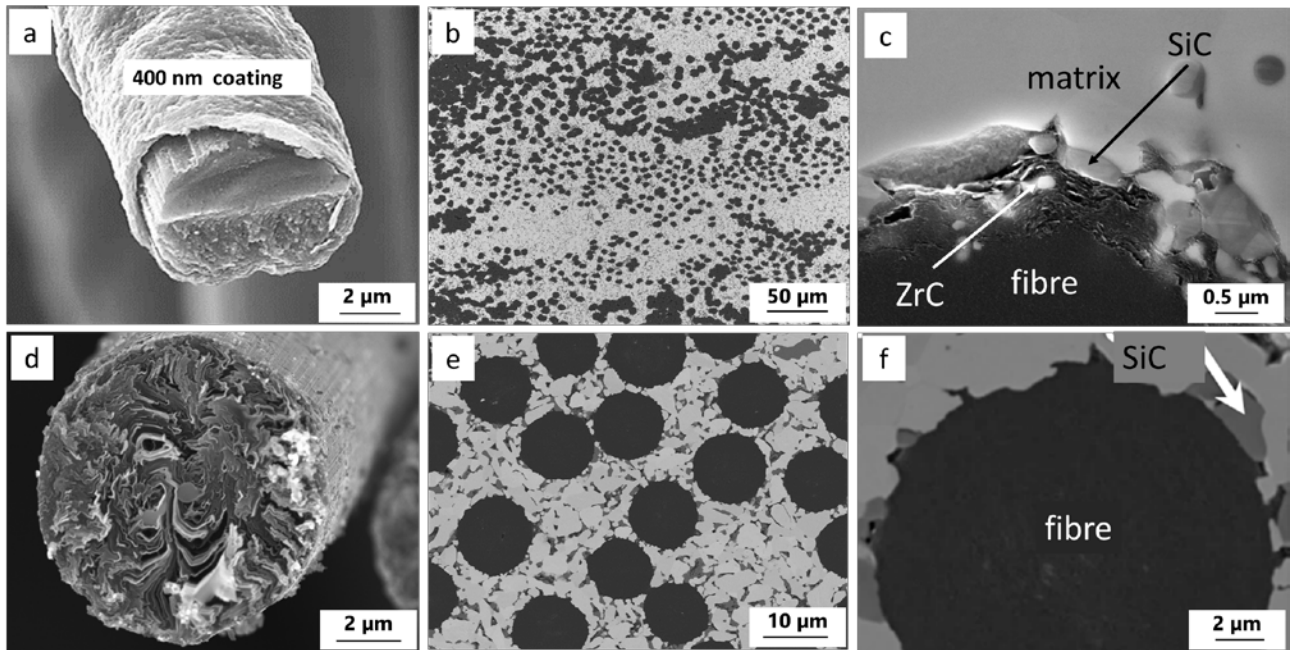


Fig. 1. Fibre features and microstructural features of the composites. a) Raw PyC-coated PAN fibre, b) polished microstructure of the PAN sample and (c) PAN fibre/matrix interface, with SiC and ZrC phases d) raw Pitch based fibre, e) polished microstructure and f) strong fibre matrix interface of the PITCH sample.

### 3.2 Mechanical properties and ablation resistance

Mechanical properties are summarized in Table 1, for PAN and PITCH samples.

Property	PAN	PITCH
Density, $\rho$ ( $\text{g/cm}^3$ )	$2.8 \pm 0.1$	$3.6 \pm 0.1$
Porosity, P (%)	~18	~5
Fibre volumetric content, FVC (%)	50-55	40-45
Longitudinal flexural strength, $\sigma_1$ (MPa)	$300 \pm 50$	$260 \pm 20$
Transverse flexural strength, $\sigma_2$ (MPa)	$25 \pm 1$	$61 \pm 13$
Interlaminar shear strength by SBS, $\tau$ (MPa)	$21 \pm 2$	> 40
Longitudinal flexural strength at $1500^\circ\text{C}$ , $\sigma_{1500^\circ\text{C}}$ (MPa)	$370 \pm 110$	$440 \pm 30$
Fracture toughness by CNB, $K_{Ic}$ ( $\text{MPa}\cdot\text{m}^{0.5}$ )	$14.6 \pm 3.0$	$8.7 \pm 0.4$
Work-of-Fracture by CNB, WoF ( $\text{kJ/m}^2$ )	$4.6 \pm 1.2$	$0.5 \pm 0.1$

Table 1: Properties of PAN and PITCH reinforced composites.

The room temperature flexural strength was higher for PAN sample owing to the higher strength of the PAN-based fibres and higher fibre volumetric content (FVC). From load-displacement curves (Fig. 2a), it can be seen that both samples suffered from interlaminar shear. Hence, the reported flexural strengths are conservative values. Transverse strength is 3 times higher for PITCH, which is related to the higher degree of compaction of the matrix. The load displacement curves however show that in this direction the sample display a brittle behaviour (Fig. 2b), i.e. after reaching the maximum load, the material collapses. Strengths in the order of 60-70 MPa were obtained with a similar composite characterized by the same type of fibre, FVC, and matrix porosity although reactive sintering was involved [22]. Investigation about strength retention in this direction showed that these composites are insensitive to flaws of about 50  $\mu\text{m}$  despite the brittle behaviour dominated by the matrix - in other words, flaws of at least 50  $\mu\text{m}$  are already present in these composites characterized by densified matrix - [22]. Analogously to the transverse strength, PAN sample was also more prone to interlaminar fracture (Fig.2 c), with interlaminar shear strength (ILSS) of 20 MPa, i.e. more than halved as compared to PICTH. On the other hand, PITCH samples did not show a dominated interlaminar shear failure and for this reason we can only state that ILSS should be higher than 40 MPa, which is the maximum interlaminar shear stress withstood during the test. Again, the lower degree of penetration of the slurry in the fibre bundles made the PAN composite more prone to delamination compared to PITCH.

The 1500°C flexural strength confirmed the general tendency of these composites, e.g. the improvement of mechanical properties with increasing temperature. For PAN sample, longitudinal strength passed from 300 to 370 MPa, for PITCH the increase was even more marked, from 255 to 440 MPa. This improvement was related to both increase of mechanical properties of Carbon fibres with temperature [23] and especially to release of thermal residual stresses developed during the densification process [24].

Measure of the fracture toughness for this kind of composites can be debateable. Commonly the SENB technique is used, however the theoretical condition of having a sharp notch is quite hard to satisfy with this technique. On the other hand, using the CNB technique, the accuracy of the chevron initial crack is much higher, but the obtained values can be slightly overestimated due to R-curve behaviour of these composites. Nevertheless, using the same technique for such different composites could at least give a term of comparison of the values. In the case of PAN sample, the average value was 14.6 MPa  $\text{m}^{0.5}$ , and the WoF was around 4.6  $\text{kJ}/\text{m}^2$  (Fig. 2e). This value was much higher than those reported in the literature that are generally lower than 2  $\text{kJ}/\text{m}^2$  [25]. For PITCH sample, the fracture toughness recorded was 8.7 MPa  $\text{m}^{0.5}$ , with a WoF of 0.5  $\text{kJ}/\text{m}^2$ . Indeed, the



characteristics of the interface, which allowed a higher pull-out in case of PAN-based fibres (Fig. 2e,f), as well as the higher content of fibres were factors explaining the higher values recorded for PAN sample. Similar results about the effect of pyrolytic carbon coating were obtained by Zhang et al. [25]. They also observed that coating promoted the fibre pull-out and led to a non-brittle fracture mode. However, owing to the more uneven fibre distribution in PAN sample, all the reported mechanical responses resulted more scattered with respect to the PITCH sample (Fig. 2d). The dispersion of values may be narrower if larger specimens are fractured, which is object of future works. Moreover, the flexural tests on larger specimens may increase the ultimate flexural stress by limiting the interlaminar shear stresses during bending moment. Hence, especially PAN specimens, which show low ILSS, may show a considerably higher flexural strength.

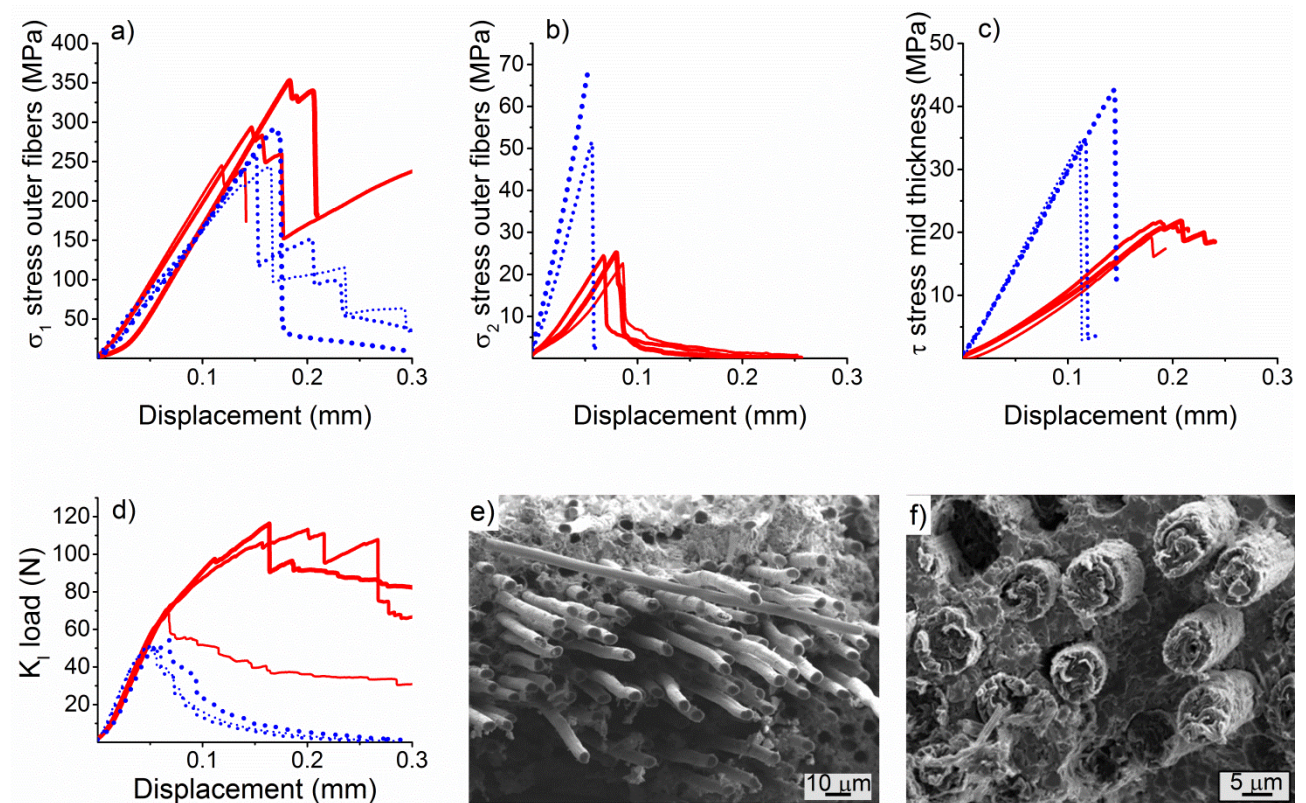


Fig. 2. Stress-displacement curves of PAN (solid curves) and PITCH (dotted curves) for a) longitudinal and b) transverse bending strength, and c) interlaminar shear strength. d) Fracture toughness load-displacement curves and related fracture surfaces of e) PITCH and f) PAN

Arc-jet tests of PAN-based composites were extensively discussed in previous papers [26][20]. All the samples tested underwent a rapid increase of the surface temperature reaching 2600-2800K, due the so-called “jump of radiance” generally observed for UHTC-based materials [27]. Visually, both sample surfaces changed their colour from the original dark grey to white, due to the oxidation of  $ZrB_2$  to  $ZrO_2$  and vaporization of grey surface silica. Although a detailed analysis of the composites microstructure is out of the scope of the present work, some considerations can be done.

For PITCH sample, the weight loss was estimated as the difference between final and initial weight, normalized to the period of time during which the sample temperature was  $>1000^{\circ}\text{C}$ , e.g. 450 s. The net weight loss was almost negligible,  $2 \cdot 10^{-4}$  g/s, and was accompanied by a slight volume expansion. On the contrary, for PAN-reinforced composites, a proper evaluation of weight and volume variations was not possible due to oxide spalling. Weight variations were due to concurrent phenomena, e.g. increase of weight due to oxidation of  $\text{ZrB}_2$  and  $\text{SiC}$  to the corresponding oxides, whilst decrease of weight was caused by Cf vaporization on the surface and/or eventual detachment of the oxidized layer from the unoxidised bulk. In the case of the PAN sample the oxide layer showed the tendency to spall-off from the bulk due to CTE mismatch with the unreacted bulk and brittleness of the oxide scale, see Figs. 3 a,b. For this composite, the higher amount of fibres, 50-55 vs 40-45 vol%, the formation of grouped fibres in the matrix, fibres joined during the coating deposition, and the presence of higher residual porosity, 18 vs 7 vol%, made it difficult for the matrix to exert its protective action. On the contrary, PITCH samples demonstrated a promising self-healing ability, testified by the capability of rapid closure of pores generated by fibre burning and good adhesion of the scale to the bulk, see Figs. 3 d,e.

The micrographs reported in Fig. 3c and Fig. 3f, confirmed the optical view, the surface oxide layer was compact in PITCH composite but cracked and discontinuous in PAN composite because borosilicate glass was not able to repair the large defects and voids left by vaporization of grouped fibres.

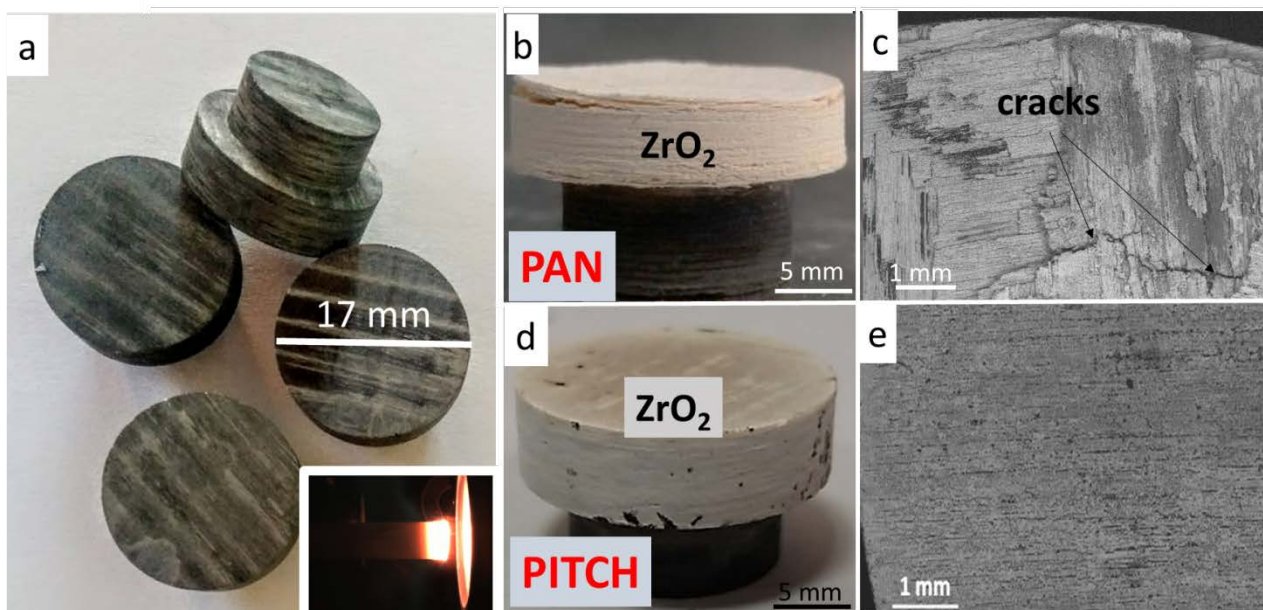


Fig. 3. a) As machined arc-jet prototypes with an inset of the test recorded by thermo-camera, b) visual appearance of PAN sample after the test showing  $\text{ZrO}_2$  spalling, c) surface microstructure detected by SEM showing oxide discontinuities and cracks. d) Visual appearance of PITCH sample after the test, e) surface microstructure by SEM.



In summary, this study highlighted that the choice of the fibre strongly affects the microstructure and final performance of UHTCMCs. First of all, the different characteristics of PyC-coated PAN and uncoated PITCH preforms affected the composite preparation, resulting in different levels of matrix homogenization, porosity and diverse fibre concentration. Similar to conventional CMCs, flexural strength and fracture toughness were positively affected by higher fibre strength, higher fibre volumetric fraction and the relatively weaker fibre/matrix interface, characteristics of the PAN reinforced composite. The use of PyC-coated PAN based fibres facilitated fibre pullout and load transfer from the matrix to the fibre. On the contrary, transverse strength, interlaminar strength and oxidation resistance were mostly influenced by the compactness of the matrix and the stronger matrix-fibre interface, characteristics peculiar of UHTCMCs developed with pitch fibres. Table 2 ultimately compares the performances of the two composites with respect to desired requirements. This study further shows that, at this stage of the progress in the material development, already a high number of requirements can be satisfied when pitch fibres are used. However, the results are promising for both types of composites and we believe there is still a high margin for improving their properties and performance.



















Desired features	PAN	PITCH
Well integrated ultra-refractory matrix (UHTC) and C fiber fabric		
Moderate density		
No fiber coating		
Low porosity to hinder penetration of corrosive/oxidative gases		
Fibre pullout at fracture – weak interface		
No environmental external coating		
Mechanical properties – Flexural strength, toughness		
High temperature properties		
Ablation resistance		

Table 2: Comparison of UHTCMC features in relation to the desired requirements.

#### 4. Conclusions

In this work we compared properties and microstructure of two UHTCMCs containing PyC-coated PAN or uncoated pitch fibres. UHTCMCs were successfully fabricated by slurry infiltration and spark plasma sintering using different type of fibres, although the final fibre volumetric amount was slightly different, but in the 40-55 range. A highly homogenous fibre dispersion was achieved with UD pitch-

based fibre fabrics, leading to low matrix porosity. The PyC coating was effective to protect PAN based fibres during sintering at high temperature, facilitating pullout and increasing the damage tolerance of the composite, but led to little microstructure inhomogeneities owing to partial gluing of the fibre bundles upon coating application. Uncoated pitch-based fibres were well anchored to the UHTC matrix, resulting in a strong interface, but the intrinsic onion structure of the fibre led to some extent of fibre pull-out.

Properties mostly determined by fibre strength and weak interface, strength and toughness, were higher if coated PAN-based fibres were used as reinforcement. Properties primarily affected by matrix density and high interface strength, transverse strength, interlaminar shear strength, and oxidation resistance, were higher for pitch-reinforced composites. The high matrix porosity and fibre content of the PAN composite were detrimental factors for the ablation resistance in arc-jet test.

### Acknowledgements

The C<sup>3</sup>HARME research project has received funding by the European Union's Horizon2020 research and innovation programme under the Grant Agreement 685594. Authors wish to acknowledge A. Schoberth (AIRBUS), P. Mittermeier (AIRBUS), F. Meistring (Arianegroup) for technical support, S. Mungiguerra and R. Savino (University of Naples) for arc-jet tests.

### Bibliography

- [1] L. Zoli, A. Vinci, P. Galizia, C. Melandri, D. Sciti, On the thermal shock resistance and mechanical properties of novel unidirectional UHTCMCs for extreme environments, *Sci. Rep.* 8 (2018) 9148. doi:10.1038/s41598-018-27328-x.
- [2] W.G. Fahrenholtz, G.E. Hilmas, I.G. Talmy, J.A. Zaykoski, Refractory diborides of zirconium and hafnium, *J. Am. Ceram. Soc.* 90 (2007) 1347–1364. doi:10.1111/j.1551-2916.2007.01583.x.
- [3] E.P. Simonenko, N.P. Simonenko, V.G. Sevastyanov, N.T. Kuznetsov, ZrB<sub>2</sub>/HfB<sub>2</sub>-SiC Ceramics Modified by Refractory Carbides: An Overview, *Russ. J. Inorg. Chem.* 64 (2019) 1697–1725. doi:10.1134/S0036023619140079.
- [4] N.P. Padture, Advanced structural ceramics in aerospace propulsion, *Nat. Mater.* 15 (2016) 804–809. doi:10.1038/nmat4687.
- [5] D. Gosset, M. Dollé, D. Simeone, G. Baldinozzi, L. Thomé, Structural evolution of zirconium carbide under ion irradiation, *J. Nucl. Mater.* 373 (2008) 123–129. doi:10.1016/j.jnucmat.2007.05.034.
- [6] C. Dickerson, Y. Yang, T.R. Allen, Defects and microstructural evolution of proton irradiated titanium carbide, *J. Nucl. Mater.* 424 (2012) 62–68. doi:10.1016/j.jnucmat.2012.02.005.
- [7] M. NAKAGAWA, Y. SUZUKI, A. CHIBA, Y. GOTOH, R. JIMBOU, M. SAIDOH, Development of Boron Carbide-Carbon Fiber Composite Ceramics as Plasma Facing Materials in Nuclear Fusion Reactor (Part 1), *J. Ceram. Soc. Japan.* 105 (1997) 851–857. doi:10.2109/jcersj.105.851.
- [8] L.M. Garrison, G.L. Kulcinski, G. Hilmas, W. Fahrenholtz, H.M. Meyer, The response of ZrB<sub>2</sub> to simulated plasma-facing material conditions of He irradiation at high temperature, *J. Nucl. Mater.* 507 (2018) 112–125. doi:10.1016/j.jnucmat.2018.04.016.
- [9] A. Bhattacharya, C.M. Parish, T. Koyanagi, C.M. Petrie, D. King, G. Hilmas, W.G.

- Fahrenholtz, S.J. Zinkle, Y. Katoh, Nano-scale microstructure damage by neutron irradiations in a novel Boron-11 enriched TiB<sub>2</sub> ultra-high temperature ceramic, *Acta Mater.* 165 (2019) 26–39. doi:10.1016/j.actamat.2018.11.030.
- [10] A. Yehia, R. Vaßen, R. Duwe, D. Stöver, Ceramic SiC/B<sub>4</sub>C/TiC/C composites as plasma facing components for fusion reactors, *J. Nucl. Mater.* 233–237 (1996) 1266–1270. doi:10.1016/S0022-3115(96)00155-9.
- [11] L.M. Rueschhoff, C.M. Carney, Z.D. Apostolov, M.K. Cinibulk, Processing of fiber-reinforced ultra-high temperature ceramic composites: A review, *Int. J. Ceram. Eng. Sci.* (2020). doi:10.1002/ces2.10033.
- [12] J. Binner, M. Porter, B. Baker, J. Zou, V. Venkatachalam, V.R. Diaz, A. D’Angio, P. Ramanujam, T. Zhang, T.S.R.C. Murthy, Selection, processing, properties and applications of ultra-high temperature ceramic matrix composites, UHTCMCs – a review, *Int. Mater. Rev.* (2019). doi:10.1080/09506608.2019.1652006.
- [13] Q. Li, S. Dong, Z. Wang, G. Shi, Fabrication and properties of 3-D Cf/ZrB<sub>2</sub>-ZrC-SiC composites via polymer infiltration and pyrolysis, *Ceram. Int.* 39 (2013) 5937–5941. doi:10.1016/j.ceramint.2012.11.074.
- [14] M. Küttemeyer, T. Helmreich, S. Rosiwal, D. Koch, Influence of zirconium-based alloys on manufacturing and mechanical properties of ultra high temperature ceramic matrix composites, *Adv. Appl. Ceram.* 117 (2018) s62–s69. doi:10.1080/17436753.2018.1509810.
- [15] L. Li, Y. Wang, L. Cheng, L. Zhang, Preparation and properties of 2D C/SiC–ZrB<sub>2</sub>–TaC composites, *Ceram. Int.* 37 (2011) 891–896. doi:https://doi.org/10.1016/j.ceramint.2010.10.033.
- [16] V. Rubio, P. Ramanujam, J. Binner, Ultra-high temperature ceramic composite, *Adv. Appl. Ceram.* (2018). doi:10.1080/17436753.2018.1475140.
- [17] L. Zoli, A. Vinci, P. Galizia, C.F. Gutiérrez-Gonzalez, S. Rivera, D. Sciti, Is spark plasma sintering suitable for the densification of continuous carbon fibre - UHTCMCs?, *J. Eur. Ceram. Soc.* (2019). doi:10.1016/j.jeurceramsoc.2019.12.004.
- [18] L. Zoli, D. Sciti, Efficacy of a ZrB<sub>2</sub>–SiC matrix in protecting C fibres from oxidation in novel UHTCMC materials, *Mater. Des.* 113 (2017) 207–213. doi:10.1016/j.matdes.2016.09.104.
- [19] S. Mungiguerra, G.D. Di Martino, A. Cecere, R. Savino, L. Silvestroni, A. Vinci, L. Zoli, D. Sciti, Arc-jet wind tunnel characterization of ultra-high-temperature ceramic matrix composites, *Corros. Sci.* (2019). doi:10.1016/j.corsci.2018.12.039.
- [20] S. Mungiguerra, G.D. Di Martino, A. Cecere, R. Savino, L. Zoli, L. Silvestroni, D. Sciti, Characterization of carbon-fiber reinforced ultra-high-temperature ceramic matrix composites in arc-jet environment, in: *Proc. Int. Astronaut. Congr. IAC*, Bremen, Germany, 2018.
- [21] P. Galizia, S. Failla, L. Zoli, D. Sciti, Tough salami-inspired Cf/ZrB<sub>2</sub> UHTCMCs produced by electrophoretic deposition, *J. Eur. Ceram. Soc.* 38 (2018) 403–409. doi:10.1016/J.JEUCERAMSOC.2017.09.047.
- [22] P. Galizia, D. Sciti, F. Saraga, L. Zoli, Off-axis damage tolerance of fiber-reinforced composites for aerospace systems, *J. Eur. Ceram. Soc.* (2019). doi:10.1016/j.jeurceramsoc.2019.12.038.
- [23] C. Sauder, J. Lamon, R. Pailer, The tensile behavior of carbon fibers at high temperatures up to 2400 °C, *Carbon N. Y.* 42 (2004) 715–725. doi:10.1016/j.carbon.2003.11.020.
- [24] P. Galizia, L. Zoli, D. Sciti, Impact of residual stress on thermal damage accumulation, and Young’s modulus of fiber-reinforced ultra-high temperature ceramics, *Mater. Des.* 160 (2018) 803–809. doi:10.1016/J.MATDES.2018.10.019.
- [25] D. Zhang, P. Hu, S. Dong, Q. Qu, X. Zhang, Effect of pyrolytic carbon coating on the microstructure and fracture behavior of the Cf/ZrB<sub>2</sub>-SiC composite, *Ceram. Int.* 44 (2018) 19612–19618. doi:10.1016/J.CERAMINT.2018.07.210.

- [26] S. Mungiguerra, G.D. Di Martino, A. Cecere, R. Savino, L. Silvestroni, A. Vinci, L. Zoli, D. Sciti, Arc-jet wind tunnel characterization of ultra-high-temperature ceramic matrix composites, *Corros. Sci.* (2019). doi:<https://doi.org/10.1016/j.corsci.2018.12.039>.
- [27] J. Marschall, D. Pejakovic, W.G. Fahrenholtz, G.E. Hilmas, F. Panerai, O. Chazot, Temperature Jump Phenomenon During Plasmatron Testing of ZrB<sub>2</sub>-SiC Ultrahigh-Temperature Ceramics, *J. Thermophys. Heat Transf.* 26 (2012) 559–572.